



Effect of coarse aggregate grading on the ASR expansion and damage of concrete



Bishnu P. Gautam, Daman K. Panesar ^{*}, Shamim A. Sheikh, Frank J. Vecchio

Department of Civil Engineering, University of Toronto, Canada

ARTICLE INFO

Article history:

Received 25 January 2016
4 July 2016
Accepted 23 February 2017
Available online xxxx

Keywords:

Alkali-aggregate reaction (C)
Expansion (C)
Aggregate (D)
Degradation (C)
Aggregate grading (author-nominated)

ABSTRACT

Assessment of alkali-silica reactivity is an important quality control measure for concrete aggregates in preventing alkali-silica reaction (ASR) in concrete structures. However, the reactivity is often assessed, by the concrete prism test as specified in ASTM C1293, for a particular grading of coarse aggregate that may deviate from the aggregate grading in field concrete. This study investigated the effects of coarse aggregate grading on the ASR expansion and damage of concrete. The results indicated that a deviation of 10% in the grading of reactive coarse aggregate could result in up to 50% larger concrete expansion compared to concrete with standard (ASTM C1293) grading. Aggregate grading also significantly influenced the ASR damage of concrete as measured by the damage rating index method. Furthermore, aggregate grading influenced the quality of concrete. Aggregate grading remains an important parameter in the study of the reactivity of aggregates and the ASR performance of concrete.

© 2017 Elsevier Ltd. All rights reserved.

1. Introduction

Reactive aggregate is a necessary component required for the occurrence of alkali-aggregate reaction which is a serious deterioration problem in concrete structures. Alkali-silica reaction (ASR), the predominant type of alkali-aggregate reaction, takes place between the alkali hydroxides available in concrete pore fluid and the reactive silica supplied by the aggregates, and causes cracking, expansion and deterioration of concrete. The type and amount of reactive silica available in aggregates largely influences their alkali-silica reactivity. The proportion and the size of a particular type of reactive aggregate have also been found to largely influence the expansive behavior of ASR-affected concrete, which are generally observed as pessimum effects [1–6].

ASR expansion of a concrete mix varies with the type, content and size of the reactive aggregate. For a particular type of reactive aggregate, a pessimum proportion is the certain proportion of reactive aggregate that corresponds to the maximum expansion [1]. Similarly, the pessimum size corresponds to the aggregate size exhibiting the maximum expansion [1]. Most of the studies on pessimum size have focused on fine aggregate. Although the exact size may vary with the type of aggregate and also with the size of the specimen [5], the pessimum size is generally observed to be in the range of 0.5–2 mm [1,3,7].

The size effect is, however, less clearly understood for coarse aggregates [8,9]. Fracture mechanics based approaches are sometimes used to explain the effect of aggregate size on ASR performance [10,11]. Gao et al. [5] proposed that the effect of aggregate size may vary relative to the size of the concrete specimen. Based on experimental observations, Zhang et al. [4] concluded that expansion is reduced with an increase in size for a reactive siliceous aggregate (from China). A similar observation of reduced expansion with an increase in aggregate size was observed by Wigum [12] for a highly reactive aggregate (from Iceland). On the other hand, Dunant and Scrivener [11] reported that the maximum expansion among the size ranges of 0–2 mm, 2–4 mm, 4–8 mm and 8–16 mm (for chloritic schist type Alpine aggregate) was observed for the size range of 4–8 mm. French [13] reported that the size range for the harshest ASR damage varies for different types of aggregates. For instance, reactive chert aggregate was most damaging in the size range of 3–7 mm, and recrystallized sandstone was most damaging in the size range of 10–20 mm. These studies indicate that the size of the coarse aggregate can influence the ASR expansion and damage of concrete. Moreover, since coarse aggregate in concrete involves a large size range, total expansion of concrete for a given aggregate grading may indeed be composed of individual contributions of different size fractions within the aggregate grading [2,11].

The gradation of coarse aggregate in concrete spans a relatively broad spectrum, usually from 5 to 25 mm. A concrete mix design usually follows a grading requirement (e. g. ASTM C33 [14]) for coarse aggregate. For instance, ASTM C1293 [15], the concrete prism test (CPT), prescribes a size range of 4.75–19.0 mm for coarse aggregate. For the size range of 4.75–19.0 mm, ASTM C1293 [15] specifies that the coarse

^{*} Corresponding author at: Department of Civil Engineering, University of Toronto, 35 St. George St., Toronto, Ontario M5S 1A4, Canada.

E-mail addresses: bgautam@gmail.com (B.P. Gautam), d.panesar@utoronto.ca (D.K. Panesar), sheikh@ecf.utoronto.ca (S.A. Sheikh), fjv@ecf.utoronto.ca (F.J. Vecchio).

aggregate be comprised of three equal proportions: 19.0–12.5 mm, 12.5–9.5 mm and 9.5–4.75 mm. In context with ASR, a specific coarse aggregate grading is necessary to provide a basis to compare CPT results from different researchers by eliminating the consequences such as the variation in aggregate grading. However, the consequences of deviating from a specified grading of reactive coarse aggregate on concrete's response to ASR have not been adequately reported in the literature.

Two aspects can be specifically identified to indicate the need for a study on the influence of the variation in aggregate grading on the ASR performance of concrete. First, most ASR studies follow a specific mix design and a specific grading of coarse aggregate, and hence, the influence of the variation in aggregate grading is inadequately understood. Concomitantly, the CPT mix as per ASTM C1293 [15] cannot represent field mixes in which the mix design and the aggregate grading are different from ASTM C1293 [15] mix design [16]. Second, maintaining a specified grading is logistically challenging for ASR studies involving large test specimens, such as slabs, walls and exposure blocks [17–20]. Large concrete test specimens require a relatively large amount of aggregate, on a scale of several tons. The challenge of adhering to a specified grading is highlighted by the fact that a study “impact of aggregate gradation on properties of Portland cement concrete” [21] was conducted recently for the South Carolina Department of Transportation with the goal to determine whether concrete containing aggregate with an out-of-specification grading should be accepted or rejected. The study [21] investigated the influence of variations in aggregate grading on selected properties of concrete, such as compressive strength, modulus of elasticity, slump, split tensile strength and rapid chloride ion permeability. The study [21] suggested that, as long as the fresh properties of concrete are acceptable, any deviation in aggregate grading by $\pm 12\%$ may be acceptable for the strength performance of concrete; however the effect of aggregate grading should be considered more seriously for the cracking and durability performance of concrete. Nevertheless, no consideration was given to the influence of aggregate grading on ASR performance.

Recently, an ASR research project required constructing several large specimens requiring some cubic meters of concrete [20]. This motivated a study to investigate the influence of coarse aggregate grading on the ASR performance of concrete. This study investigates the influence of aggregate grading on the expansion and damage of concrete due to ASR. Three mixes of concrete are compared with the primary variable being the coarse aggregate grading as: a standard composition as per ASTM C1293 [15]; a fine-dominant composition; and a coarse-dominant composition.

The investigation involves concrete prisms which were measured for expansion as per ASTM C1293 [15]. The prisms were tested for modulus of rupture, surface resistivity, and damage rating index at different ages from 28 to 365 days. In addition, a number of concrete cylinders were tested for compressive strength, modulus of elasticity, and ultrasonic pulse velocity (UPV) at different ages from 28 to 365 days. This paper presents the findings from these measurements to better understand the influence of aggregate grading on the alkali-silica reactivity of concrete. The effect of grading on the quality of concrete is also discussed. The importance of grading and the possible consequences of deviating from a standard grading are highlighted.

2. Materials and methods

2.1. Coarse aggregate grading

The grading for the CPT as specified by ASTM C1293 [15] was taken as the standard grading. This study captures practical scenarios of likely deviations of the coarse aggregate grading compared to the specified ASTM C1293 [15] grading. Rangaraju et al. [21] suggested that an acceptable deviation in aggregate grading can be as large as $\pm 12\%$ based on the strength performance of the concrete. This study considered a similar deviation in aggregate grading of $\pm 10\%$. Even though several

combinations of aggregate gradings are possible by varying the relative proportions of the smaller size fractions of aggregate particles [11], for simplicity, three different gradings were considered in this study as depicted in the aggregate gradation curves in Fig. 1. The three gradings are described as:

- i) Standard grading: as specified in ASTM C1293 [15], which consisted of 33.33% (by mass) each of the three size ranges of coarse aggregate, namely, a) 19.0–12.5 mm, b) 12.5–9.5 mm, and c) 9.5–4.75 mm;
- ii) Fine-dominant grading: which consisted of 10% (by mass) less of the coarser fraction and 10% excess of the finer fraction compared to the standard grading; and
- iii) Coarse-dominant grading: which consisted of 10% (by mass) excess of the coarser fraction and 10% less of the finer fraction compared to the standard grading.

The overall size range of 19.0–4.75 mm was maintained for all gradings.

2.2. Materials and concrete mix design

In general, all mixes were based on the CPT as per ASTM C1293 [15]. The three concrete mix designs are shown in Table 1. The primary difference between the three mixtures is the coarse aggregate grading. Accordingly, the three mixes were designated as the standard mix (mix S), fine-dominant mix (mix F) and coarse-dominant mix (mix C).

Spratt aggregate was used as the reactive coarse aggregate. It is a siliceous limestone, crushed aggregate from a quarry near Ottawa, Ontario, Canada, and has been used as a reference aggregate to calibrate ASR test methods [22]. Except for ASR, the aggregate meets the normal physical requirements for concrete aggregate [17]. The Los Angeles Abrasion value for Spratt aggregate was reported as 19% [23]. The specific gravity of the aggregate at oven-dry condition was 2.68 and the absorption was 0.5%.

The non-reactive fine aggregate was natural sand from Orillia, Ontario, Canada. The water-to-cement ratio was 0.44 for all mixes. High alkali general use (GU) cement was used with a total alkali content of 0.99% Na₂O equivalent by mass of cement. The chemical composition of cement is shown in Table 2. The alkali level of the concrete mixes was increased to 5.25 kg Na₂O equivalent per m³ of concrete by adding NaOH pellets to water prior to concrete mixing.

2.3. Casting and conditioning of the specimens

Concrete prisms were cast as per ASTM C1293 [15]. Nine prisms and nine cylinders were cast from mix F and mix C. For mix S, two batches of concrete were used for casting concrete specimens. The first batch was

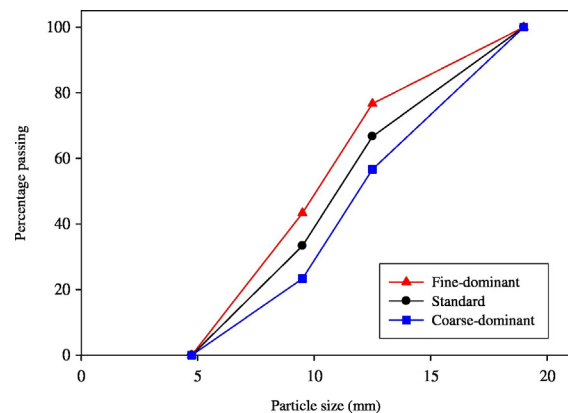


Fig. 1. Coarse aggregate grading scenarios.

Table 1
Mix designs of concrete.

Mix (coarse aggregate grading)	Cement (kg/m ³)	Water (kg/m ³)	Coarse aggregate (kg/m ³)			Sand (kg/m ³)	NaOH pellets (kg/m ³)
			19.0–12.5 mm	12.5–9.5 mm	9.5–4.75 mm		
S (standard)	420	184.8	371.67	371.67	371.67	719.2	1.41
F (fine-dominant)	420	184.8	260.17	371.67	483.17	719.2	1.41
C (coarse-dominant)	420	184.8	483.17	371.67	260.17	719.2	1.41

Note: the dry-rodded density of coarse aggregate for the standard grading was 1585 kg/m³. The mass of aggregates is shown for saturated surface-dry condition.

used to cast eighteen prism specimens and three cylinder specimens. The second batch was used to cast fifteen cylinders.

The size of the prism specimens was 285 mm by 75 mm by 75 mm and that of the cylinders was 100 mm (diameter) by 200 mm (height). Specimens were demolded after one day of casting. After demolding, three cylinder specimens from each batch of mix S and one cylinder each from mix F and mix C were stored in a fog room maintained at room temperature (23 ± 3 °C). Remaining specimens were stored in hermetically sealed plastic pails and were conditioned under a constant temperature of 38 ± 2 °C and relative humidity greater than 95%. Prior to performing the tests on the specimens, the pails were acclimatized at room temperature for 16 to 20 h.

2.4. Test details

2.4.1. Prisms

The concrete prisms were tested for longitudinal expansion, modulus of rupture, damage rating index (DRI), and surface resistivity. The initial reading for the longitudinal expansion of the prisms was taken at the age of one day. The prisms were subsequently measured for the longitudinal expansion at ages of 7, 28, 56, 91, 182, 273 and 365 days. The prisms were tested for modulus of rupture at ages of 28, 91, 182 and 365 days. Two prisms were tested by third-point loading as outlined in ASTM C78 [24].

The DRI method was originally proposed by Grattan-Bellew in 1995 [25] to characterize the damage in concrete suffering from ASR. Having a magnification level large enough to capture the micro-cracks but small enough to cover the heterogeneity of concrete, DRI is a microscopic method that quantitatively assesses the extent of ASR damage in concrete. The DRI method involves the judgment of an observer in classifying the different damage features and thus can involve some variability. In an attempt to minimize such variability, a revised version of the DRI method was proposed by Villeneuve et al. [26], which was adopted in this study. The method involves counting seven petrographic features that are shown, along with their weighting factors, in Table 3. Further reference to DRI analysis was made to the detailed guidelines on DRI published by Fournier et al. [27].

The DRI was analyzed on two prism specimens at each test age. For each prism, one slice (75 mm × 75 mm) near the middle and one slice near the end were taken and polished for examination under a stereo binocular microscope at ~16× magnification. The DRI value for concrete at an age was obtained as the average for four slices from two prisms.

Electrical resistivity measurement appears as a promising tool for the performance assessment of concrete [28]. For instance, surface resistivity test was proposed as an electrical indicator of concrete permeability by the Florida Department of Transportation in 2004 [29]. The method uses a surface resistivity meter with a four-point Wenner array probe. The equipment estimates the resistance of concrete from the ratio of the potential difference between the two inner electrodes

and the current flowing between the outer electrodes [30]. Surface resistivity of concrete is calculated based on this resistance.

Surface resistivity of water-saturated concrete was strongly correlated to the bulk diffusion test [31] results and rapid chloride permeability test [32] results [30,33]. The surface resistivity ranges of 11.7–20.6 and 20.6–141.1 kΩ-cm in a semi-infinite concrete surface have, respectively, been regarded to represent “low” and “very low” chloride ion permeability with equivalent coulombs passed in the rapid chloride permeability test [32] as 1000–2000 and 100–1000, respectively [30].

In this study, surface resistivity was measured on concrete prism surfaces using a 38 mm spacing model of Resipod, a surface resistivity meter by Proceq SA Company. As the resistivity is largely influenced by the saturation [28], resistivity was measured as the first measurement on the prisms after taking them out from the plastic pails. The condensed water drops on the prism surface were wiped by a piece of cloth. For consistency, only the surface opposite to the formed surface was considered for the resistivity measurement. The resistivity of a surface was reported as an average of at least five consecutive measurements. Surface resistivity at an age was taken as an average of three prisms.

2.4.2. Cylinders

The cylinders conditioned at 38 °C were non-destructively tested for UPV in accordance with ASTM C597 [34]. UPV was measured along the longitudinal axis of the cylinders using “Pundit Lab+” equipment from Proceq USA, Inc. The cylinders were destructively tested for static modulus of elasticity in accordance with ASTM C469 [35] and compressive strength in accordance with ASTM C39 [36] at 28, 91, 182 and 365 days. The cylinders conditioned at 23 °C were tested for the static modulus of elasticity [35] and the compressive strength [36] at an age of 28 days.

3. Results and discussions

3.1. Longitudinal expansion

Longitudinal expansions of the concrete prisms for the three mixes are presented in Table 4. Since two prisms were destructively tested at each test date, the number of prisms used for expansion measurement gradually decreased over time. Therefore, each expansion result shown in Table 4 represents the average of a varying number of prisms. For mix S, the expansion at 7 days and 365 days represents the average of eighteen prisms and six prisms, respectively. For mix F and mix C, the concrete expansion at 7 days and 365 days represents the average of nine prisms and three prisms, respectively.

The expansion for mix F was significantly greater than that for mix S by approximately 50% at all ages ranging from 91 to 365 days. For mix C, designed with relatively coarser aggregates, the expansion was consistently slightly greater than that of mix S. The expansion for mix C ranged from 2 to 15% greater than the expansion for mix S at all ages except 7

Table 2
Chemical composition of GU cement.

Constituents	LOI	SiO ₂	Al ₂ O ₃	Fe ₂ O ₃	CaO	MgO	SO ₃	Alkali (Na ₂ O _{eq})	Free lime	Insoluble residue
Percentage	2.27	19.25	5.33	2.41	62.78	2.36	4.01	0.99	1.29	0.52

Table 3
Features counted in an individual grid as per the DRI method [26].

Petrographic features	Weighting factors
Closed/tight cracks in coarse aggregate particle	0.25
Opened cracks or network cracks in coarse aggregate particle	2
Cracks or network cracks with reaction product in coarse aggregate particle	2
debonded coarse aggregate	3
Disaggregated/corroded aggregate particle	2
Cracks in cement paste	3
Cracks with reaction product in cement paste	3

and 28 days. Based on the Student's *t*-test performed at a 95% confidence level, the expansion for mix C was statistically significantly greater than the expansion for mix S at all ages ranging from 56 to 365 days except at 273 days. The influence of aggregate grading on ASR expansion will be further discussed in Section 3.8.

Table 4 shows the coefficient of variation of the expansion measurements for the prism specimens of the three mixes. The coefficient of variation was less than 6% for the mix S specimens after 56 days (the large coefficient of variation before 56 days is attributed to the extremely small length changes). In comparison to the mix S specimens, larger coefficients of variation were generally observed for the mix F and mix C specimens.

The statistically significant difference between the expansions of the mix S prisms and the mix F or mix C prisms highlights the importance of grading in performing CPT or other expansion tests. It also indicates that an error in grading could be one of the factors that may cause variations in expansion results among different studies, including multi-laboratory studies.

3.2. Damage rating index

Fig. 2 shows the results of DRI analysis from 28 to 365 days for the three concrete mixes. As expected, all mixes showed an increase in DRI value with age. Statistically significantly greater values of DRI were observed for mix F and mix C in comparison to mix S. However, the greatest DRI was always observed for mix F. A contributing factor for the greatest DRI value for Mix F is that the DRI method involves counting the number of cracks which becomes greatest for mix F containing the greatest number of reactive coarse aggregate particles for the same mass of reactive coarse aggregate as with mix S and mix C. The DRI value for mix S increased from 123 at 28 days to 614 at 365 days. For mix F, the DRI value increased from 238 at 28 days to 1411 at 365 days. The DRI value for mix C increased from 191 at 28 days to 1157 at 365 days. DRI values for the fine-dominant and coarse-dominant concrete mixes were, respectively, 86 to 130% and 56 to 98% larger compared to the standard mix.

Table 4
Mean longitudinal expansion and coefficient of variation for the concrete prisms from the three mixes.

Age (days)	Mean longitudinal expansion (%)			Coefficient of variation (%)			No. of specimens		
	Mix S	Mix F	Mix C	Mix S	Mix F	Mix C	Mix S	Mix F	Mix C
1	0.000	0.000	0.000	–	–	–	18	9	9
7	0.003	0.006	0.002	79.0	64.3	126.6	18	9	9
28	0.013	0.009	0.008	20.0	67.2	68.2	16	9	9
56	0.048	0.060	0.055	6.0	12.5	27.9	14	7	7
91	0.101	0.153	0.116	5.0	5.3	24.2	12	7	7
182	0.171	0.252	0.192	4.0	9.3	12.7	10	5	5
273	0.210	0.315	0.215	4.0	12.9	2.6	8	3	3
365	0.223	0.350	0.242	6.0	6.5	3.9	6	3	3

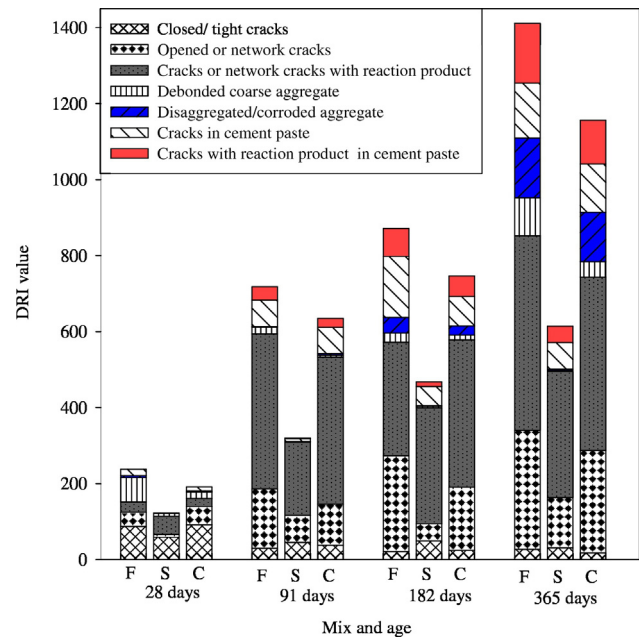


Fig. 2. DRI and the contribution of the seven features of DRI from the three mixes conditioned at 38 °C.

The damage was initiated in the reactive aggregates, and the damage initiation was predominantly in the form of 'closed/tight cracks' in the aggregates. The contribution of 'closed/tight cracks' to the DRI value decreased from 28 to 365 days for all mixes. In terms of the relative contributions of the seven features of DRI, as shown in Table 3, for all mixes the contribution of 'closed/tight cracks' to the DRI value was 37–48% at 28 days but diminished to 2–5% by 365 days. The contribution of 'opened cracks' was consistently larger in mix F than in the other two mixes. The contributions of 'debonded aggregate' and 'disaggregated particles' were relatively larger in mix F and mix C compared to mix S. The contribution to the DRI value by the cracks in cement paste, with and without reaction product, was greatest in mix F and least in mix S. The combined contribution of the two types of paste cracks ('cracks in cement paste' and 'cracks with reaction product in cement paste') consistently increased from 28 to 365 days for all three mixes. The DRI values associated with paste cracks increased from 0 to 113 for mix S, from 17 to 302 for mix F, and from 11 to 242 for mix C. In terms of the percentage contribution to the DRI value, the increase in paste cracks' contribution from 28 to 365 days was from 0 to 18%, 7 to 27% and 6 to 21%, respectively, for mix S, mix F, and mix C.

A large difference was observed among the DRI values for the three mixes with three gradings of reactive coarse aggregate. Thus, the variation in aggregate grading, despite no other changes in the mix design of concrete, was seen to influence the ASR damage of concrete. Mix F exhibited greater damage than mix C.

Fig. 3 compares the evolution of expansion and DRI in the prism specimens for the three mixes. Both the expansion and the DRI values increased with age and the overall trend of expansion and DRI were similar. Comparisons of expansion and DRI results demonstrate that any deviation in aggregate grading from the standard grading increases the expansion and damage due to ASR. However, markedly greater increases in expansion and DRI values were observed when deviating the aggregate grading towards the finer side. The expansion and DRI values were consistently the lowest for mix S and the greatest for mix F.

3.3. Modulus of rupture

Fig. 4 shows the modulus of rupture of the concrete prism specimens from the three mixes with three different gradings of reactive coarse

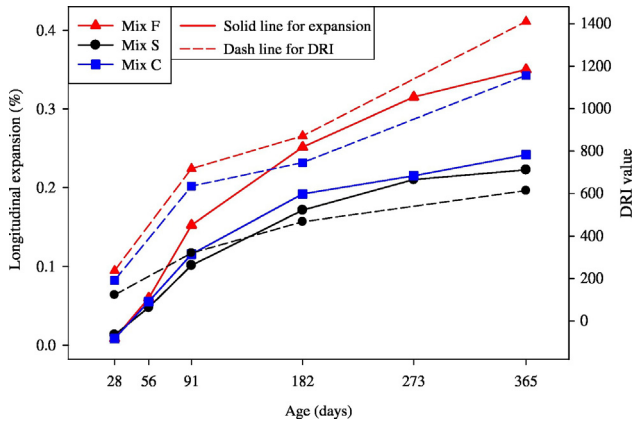


Fig. 3. Evolution of expansion and DRI with age from the three mixes conditioned at 38 °C.

aggregate. The modulus of rupture from 28 to 182 days for both mix F and mix C was less than that for mix S. While the 28-day value was approximately equal (within 2%) for the mix F and mix C specimens, it was approximately 30% lower when compared to the mix S specimens. The lower modulus of rupture, particularly at 28 days, for mix F and mix C compared to mix S indicates that any deviation in aggregate grading from the standard grading may adversely affect the flexural strength of concrete mix.

With exposure to 38 °C and greater than 95% relative humidity, the modulus of rupture was markedly affected by ASR for all mixes. Most of the reduction in the modulus of rupture occurred within 91 days when ASR expansion was less than 50% of the one-year expansion (the expansions for mix S, mix F and mix C were, respectively, 0.101%, 0.153% and 0.116% at 91 days and 0.223%, 0.350% and 0.242% at one year). This is attributed to the fact that the reduction in modulus of rupture is due to micro-cracking that can occur even before expansion [37]. However, there was no linear trend for the reduction in modulus of rupture with age. In fact, the maximum reductions in modulus of rupture were observed at various ages depending on the mix designs. The maximum reduction occurred in 91 days, 182 days and 365 days, respectively, for the mix F, mix C and mix S specimens. With reference to the 28-day value, the maximum reduction in modulus of rupture was 60% for mix F, 58% for mix S, and 53% for mix C. The largest and the most rapid reduction occurred in the mix F specimens. The mix C specimens had a slightly smaller reduction in the modulus of rupture perhaps due to increased interlocking provided by the coarse aggregates. The modulus of rupture values for all three mixes were approximately equal at the age of one year.

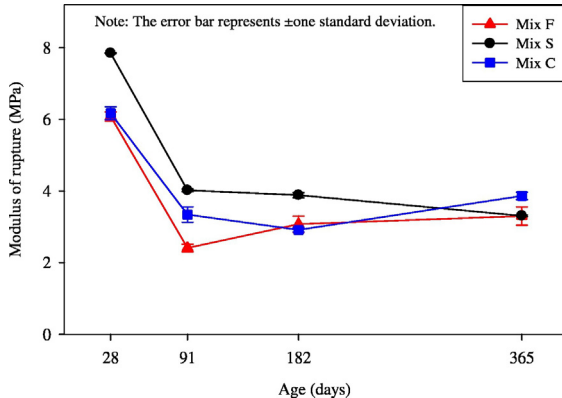


Fig. 4. Modulus of rupture of concrete prisms from the three mixes conditioned at 38 °C.

3.4. Modulus of elasticity

Cylinders were tested to evaluate the modulus of elasticity of three concrete mixes before ASR took place. The 28-day modulus of elasticity of a reference cylinder conditioned at room temperature (23 °C) was 37 GPa for mix F and 38 GPa for mix C. Similarly, for the three cylinders conditioned at 23 °C and tested at 28 days, the average modulus of elasticity for mix S was 39.6 GPa (standard deviation of 1.4 GPa). Although a limited number of cylinders did not allow for a statistical comparison, the results indicate that, due to the variation in aggregate grading considered in this study, no significant variation in modulus of elasticity was observed before ASR.

The modulus of elasticity of cylinder specimens from the three mixes is compared in Fig. 5. For all three mixes, the 28-day modulus of elasticity for the cylinders conditioned at 38 °C was smaller than the corresponding value for the cylinder conditioned at 23 °C, thus, indicating that the static modulus of elasticity was affected by ASR since its initiation. The maximum reduction in the modulus of elasticity was observed at 182 days when the reduction with respect to the reference value at 28 days was 36%, 31% and 34%, respectively, for mix F, mix S and mix C. The greatest degradation occurred for mix F and the lowest degradation occurred for mix S. The modulus of elasticity for mix F was always smaller than for mix C even though it was not statistically significant at a 95% confidence level. Relatively lower degradation in the modulus of elasticity for mix S suggests that the degradation in the modulus of elasticity is sensitive to aggregate grading. Equal proportions of the three size fractions of coarse aggregate in mix S helped to produce a concrete microstructure that was relatively more resistant to the ASR degradation compared to mix F and mix C.

3.5. Compressive strength

For cylinders conditioned at 23 °C, the 28-day mean compressive strengths values were: 35.1 MPa for mix F, 39.0 MPa for mix S (first batch), 38.8 MPa for mix S (second batch) and 42.1 MPa for mix C. Fig. 6 presents the cylinder compressive strength values for specimens conditioned at 38 °C. The compressive strength of mix F was statistically significantly smaller than the compressive strength of mix C at all ages, based on a *t*-test at 95% confidence level. On average, the mix C specimens were 14 to 25% stronger than the mix F specimens. Irrespective of the ASR, the consistently larger strength of mix C than mix F may be due to the strength enhancement by the larger (19.0–12.5 mm) aggregates, which had the largest proportion in mix C. This is supported also by the comparison between mix C and mix S at 28 and 91 days.

Compared to the 28-day strength of cylinders conditioned at 23 °C, the same-aged cylinders conditioned at 38 °C showed an increased

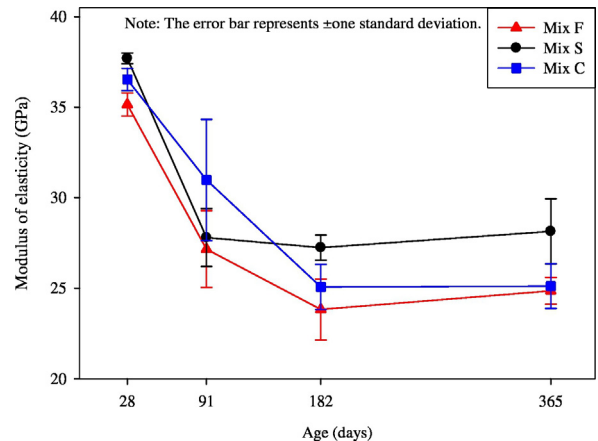


Fig. 5. Static modulus of elasticity of concrete cylinders from the three mixes conditioned at 38 °C.

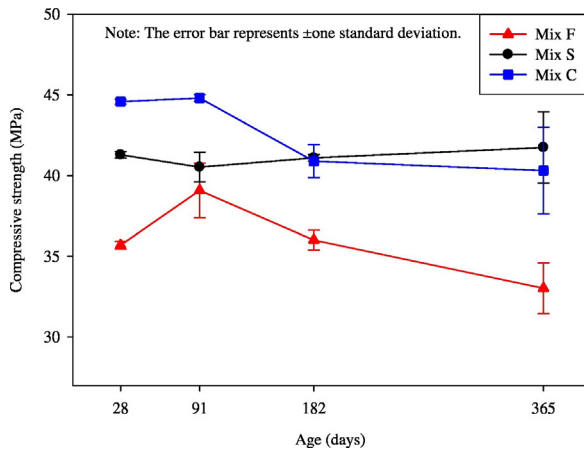


Fig. 6. Compressive strength of concrete cylinders from the three mixes conditioned at 38 °C.

compressive strength. Upon further conditioning at 38 °C, while the compressive strength of mix S remained fairly constant from 28 to 365 days, the compressive strength of mix F and mix C increased until 91 days and decreased thereafter. An initial increase in compressive strength for lower expansion followed by a reduction in compressive strength corresponding to a greater expansion has also been previously observed [38]. With respect to the 28-day compressive strength of the cylinders conditioned at 23 °C, the maximum reduction of 6% for mix F and 4% for mix C was observed at 365 days. On the other hand, an increase of 7% was observed for mix S in a similar comparison. Mix S, having relatively uniform microstructure with standard grading of coarse aggregate, did not show any degradation in compressive strength due to ASR. Mix F and Mix C, with $\pm 10\%$ deviation in coarse aggregate grading compared to mix S, showed a degradation in compressive strength due to ASR. While the extent of reduction is small and the trend of reduction is similar for both mix F and mix C, both the compressive strength and its reduction appear more sensitive to the mix dominated with relatively finer aggregate than for the mix dominated with relatively coarser aggregate.

3.6. UPV of cylinders

Fig. 7 compares the UPV of concrete over time as measured in the cylinders from the three mixes. Even though the difference in UPV was not statistically significant at 95% confidence level, UPV was always smaller for mix F than for mix C. The UPV for mix S was mostly intermediate to those of mix F and mix C. UPV for all mixes increased from 28 to

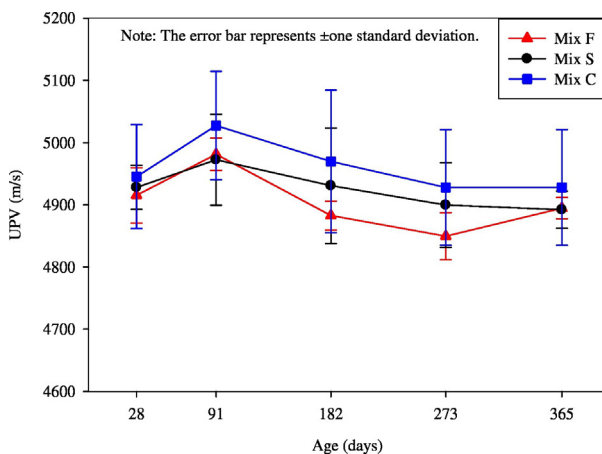


Fig. 7. UPV of concrete cylinders from the three mixes conditioned at 38 °C.

91 days but decreased thereafter. A slightly larger decrease was observed for mix F than for mix C. However, the decrease in velocity over time was not significant. UPV method does not appear to be very sensitive for monitoring the ASR damage of laboratory concrete specimens, as also reported in [39,40].

3.7. Surface resistivity

Table 5 presents the surface resistivity of prism specimens from the three mixes from one month to one year of conditioning at 38 °C. Surface resistivity of mix F was always statistically significantly smaller compared to mix C. Even though not a direct measure of permeability, the lower resistivity of mix F consequently indicated that the mix dominated with relatively finer aggregate was more permeable [28] than the mix dominated with relatively coarser aggregate. The higher permeability of mix F compared to mix C is partly attributed to the greater DRI value of mix F compared to mix C as presented in Section 3.2.

For mix S, the surface resistivity was intermediate to that of mix F and mix C until 3 months, but was slightly larger than for both mix F and mix C after 3 months. While the surface resistivity was not improved with age for mix F and mix C specimens, mix S specimens showed a slight increase in the surface resistivity. This indicates that the microstructure of mix S, having equal proportions of the three size ranges of coarse aggregate, assisted in limiting the extent of ASR cracks and consequently limiting the connectivity of cracks when compared to mix F and mix C. This observation is in agreement with the DRI results that the lowest DRI was always observed for mix S.

The variation in surface resistivity among the three mixes was quite small. For comparison, Table 5 also shows the surface resistivity measurements performed on identical concrete prisms of a non-reactive concrete mix which was made by substituting the reactive coarse aggregate in mix S by non-reactive limestone aggregate. As shown in Table 5, the resistivity of the non-reactive concrete was markedly greater than the resistivity of the three reactive concrete mixtures. Compared to the magnitude of difference between the reactive and non-reactive concrete, the difference among the three mixes is quite negligible.

The variation in surface resistivity of the three reactive mixes with age was also quite small. In contrast, an increasing trend with age was observed in the surface resistivity of the non-reactive mix. While continued hydration is believed to cause the increasing trend, no such clearly increasing trend in the reactive concrete indicates an increasing effect of ASR cracking.

Finally, it should also be noted that resistivity is largely influenced by the degree of saturation and the temperature of concrete. An increase in temperature by 1 °C can reduce the electrical resistivity of concrete by 3% and an increase in the degree of saturation by 1% can also reduce the electrical resistivity of concrete by 3% [41]. Similarly, the evolution in concrete resistivity may be sensitive to the curing temperature [42]. These factors indicate that the surface resistivity test may have limited applicability, particularly in evaluating ASR-affected concrete structures.

Table 5

Surface resistivity of concrete prisms from the three reactive mixes and one non-reactive mix conditioned at 38 °C.

Age (day)	Mix F		Mix S		Mix C		Non-reactive mix	
	Average	St. dev.	Average	St. dev.	Average	St. dev.	Average	St. dev.
28	12.6	0.9	13.8	0.4	15.0	1.2	21.2	0.7
56	12.1	0.8	14.0	0.5	15.1	1.2	28.5	0.9
91	13.0	0.6	13.4	0.4	15.5	0.5	31.5	1.4
182	12.5	0.7	17.9	0.6	14.4	0.4	36.8	1.7
273	13.1	0.4	15.3	0.6	14.5	0.9	44.0	1.2
365	10.6	0.6	18.2	0.4	12.6	1.1	46.3	0.1

3.8. Discussion on the effect of grading

The comparison of ASR expansion of concrete made with different gradings showed a pronounced impact of aggregate grading. The deviation towards a fine-dominant grading resulted in a substantially greater expansion in as early as 91 days and remained consistently greater thereafter to reach 0.35%. A deviation in specified grading by 10% could result in 50% deviation in the ASR expansion. Keeping the same mass of reactive aggregate but of finer size allows for a greater number of smaller aggregate particles resulting in an increased number of reaction sites available for the ASR. However, mix C, with coarse-dominant grading, also showed increased expansion and DRI value compared to mix S with standard grading. Compared to mix S, the modulus of rupture of mix F and mix C specimens from 28 to 182 days was lower by 17 to 40%. Moreover, both Mix F and mix C had pronounced degradation in the compressive strength and modulus of elasticity compared to mix S. Therefore, greater expansion for both mix F and mix C than for mix S suggests that rather than the effect of the exposure of more reaction sites, the change in concrete matrix associated with the deviation in aggregate grading from the standard grading was more influential to the expansion of concrete.

Based on the tests of concrete properties, mix F had lower mechanical properties compared to mix C. Mix F had lower modulus of elasticity, UPV, surface resistivity and statistically significantly lower compressive strength. Similarly, the reductions in modulus of rupture, modulus of elasticity and compressive strength were larger for mix F than for mix C. For a particular level of expansive pressure, a lower modulus of elasticity allows concrete to undergo larger deformation and a lower tensile strength (indicated by the modulus of rupture) allows concrete to experience more cracking. Moreover, the relatively fewer larger particles in mix F are expected to have resulted in relatively less interlocking effect associated with the coarse aggregates. Similarly, the higher permeability of mix F, as indicated by the lower surface resistivity, is expected to have contributed to the relatively earlier and most damaging ASR in mix F. These mechanisms are intuitively in agreement with the markedly larger expansion of the mix F specimens compared to the mix C specimens.

Fig. 8 illustrates the cracks in two concrete slices taken from the concrete prisms from mix F and mix C after 91 days of casting. Concrete slices prepared for DRI analysis were vacuum impregnated with epoxy containing a fluorescent dye after performing DRI analysis. The surfaces after epoxy impregnation were polished again just to remove the epoxy veneer (some leftover epoxy can be seen near the bottom corners in Fig. 8b). Images were taken under a stereo-binocular microscope at 10× magnification using ultraviolet (UV) light as the source of illumination and were stitched together by using a plugin [43] available in “Fiji”

software. After stitching, the green channel of the image was extracted and converted into a greyscale image. Brightness and contrast were adjusted. It should be noted that epoxy was not able to penetrate all the cracks as the polished surfaces had contained a number of ‘filled cracks’. However, relatively longer cracks are evident in mix F (Fig. 8a) compared to mix C (Fig. 8b). It is believed that the relatively coarser aggregate in mix C contributed in intercepting cracks compared to mix F. Long cracks in mix F mostly followed along the debonded aggregate (Fig. 8a), which were always most abundantly observed in mix F as shown in Fig. 2. The debonded aggregate in mix F served as the basis which eventually led to the formation of long cracks that extended to the paste matrix from the aggregate cracks.

A slightly larger expansion (for mix C than for mix S) but a markedly larger DRI value and generally lower mechanical properties indicate that the ASR damage is revealed more effectively by the DRI method than by expansion measurement. Expansion is the external manifestation of the internal chemical reaction. It cannot effectively reveal the influence of the skeleton of concrete which is governed by the coarse aggregate. However, the DRI method assesses the interior of concrete, and thus, portrays the ASR damage more precisely.

Large variations in the expansion and damage of concrete were observed by merely varying the aggregate grading while having an identical paste volume and an identical proportion of reactive coarse aggregate. Hence, the grading of coarse aggregate should be regarded as an important parameter in the study of the reactivity of aggregate and the ASR performance of concrete.

4. Summary and concluding remarks

This study investigated the effects of variation in the grading of reactive coarse aggregate, Spratt, on the ASR expansion and damage of concrete. Three mixes of reactive concrete were studied by considering three coarse aggregate gradings, namely: 1) a standard grading with 33.33% each of the three size ranges, a) 19.0–12.5 mm, b) 12.5–9.5 mm, and c) 9.5–4.75 mm, as per ASTM C1293 [15]; 2) a fine-dominant grading which consisted of 10% less of the coarser fraction and 10% excess of the finer fraction compared to the standard grading; and 3) a coarse-dominant grading which consisted of 10% excess of the coarser fraction and 10% less of the finer fraction compared to the standard grading.

A deviation in specified grading of coarse aggregate by 10% towards the finer size resulted in 50% deviation in the expansion measurement compared to the standard mix. DRI results demonstrated that any deviation in aggregate grading from the standard grading significantly increases the damage due to ASR. DRI values for the fine-dominant and coarse-dominant concrete mixes were, respectively, 86 to 130% and

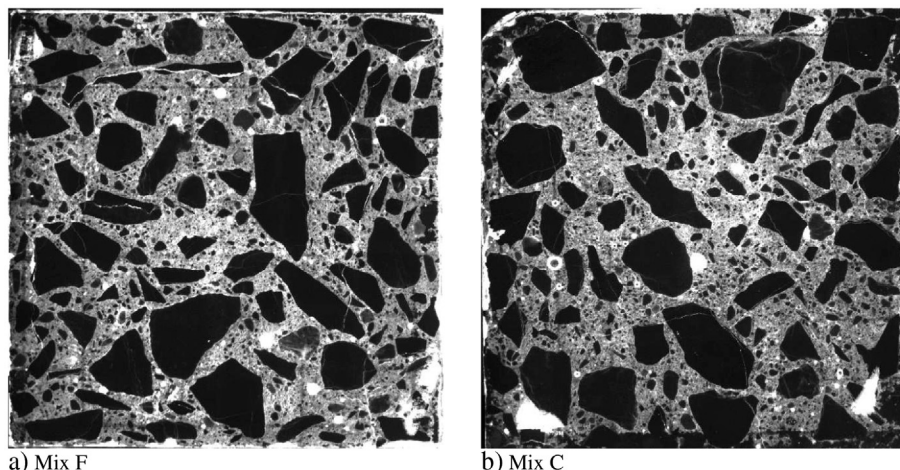


Fig. 8. UV images of the polished surfaces of concrete prisms after 91 days of casting (the surfaces are 75 mm × 75 mm).

56 to 98% larger compared to the standard mix. Also, more 'paste cracks' were observed in the prisms made of fine-dominant mix compared to the standard mix.

Over a one-year duration, the modulus of rupture of the reactive concrete prisms was reduced due to ASR by 53–60%, irrespective of the type of coarse aggregate grading used. However, an earlier and faster reduction occurred for the fine-dominant mix. The coarse-dominant mix showed a slightly smaller reduction in the modulus of rupture indicating increased interlocking provided by the coarse aggregates.

The static modulus of elasticity was affected since the onset of ASR. The maximum reduction in the modulus of elasticity of the fine-dominant, the standard, and the coarse-dominant mixes was 36%, 31% and 34%, respectively. Equal proportions of the three size fractions of coarse aggregate helped in producing a concrete microstructure that was relatively more resistant to the ASR degradation compared to the mixes with deviations in aggregate grading.

Prior to the onset of ASR, the compressive strength for the coarse-dominant mix was the largest among the three mixes indicating that the larger aggregates helped in enhancing the strength of concrete. While the mix with equal proportions of the three size fractions of coarse aggregate, mix S, did not show any degradation in compressive strength, ASR degradation in compressive strength was observed when the aggregate grading was deviated either on the finer or the coarser side.

Compared to the UPV of the coarse-dominant mix, the UPV of the fine-dominant mix was always smaller and showed larger reduction due to ASR. However, UPV appears not so sensitive for studying the ASR degradation of laboratory specimens.

Surface resistivity of concrete indicated that the fine-dominant grading resulted in a mix that was more permeable than the coarse-dominant mix. Higher permeability promoted relatively earlier and larger damage due to ASR. Equal proportions of the three size ranges of coarse aggregate assisted in limiting the extent of ASR cracks and consequently limiting the connectivity of cracks when compared to the unequal proportions of the three size ranges.

As revealed by the expansion measurements, DRI and various properties of the three concrete mixes, the variation in the coarse aggregate grading alone significantly influenced the microstructure, ASR expansion and damage of concrete. The fine-dominant grading exhibited poorer performance than the coarse-dominant grading. The findings highlight the importance of grading in performing CPT or other studies investigating the ASR performance of concrete mixtures, and also in minimizing the ASR expansion of concrete structures. The quality control in maintaining a specified grading of coarse aggregate should be stringent. Even though a deviation of $\pm 12\%$ may be acceptable for the strength performance of concrete [21], the implications are significant in a project associated with assessing the ASR performance of concrete.

Any deviation in coarse aggregate grading on either side of the standard ASTM C1293 [15] grading resulted in more expansion and more damage. This observation indicates that aggregate that is concluded as innocuous based on the concrete prism test, such as ASTM C1293 [15], may still show marked expansion and damage in concrete members in which the aggregate grading is widely different from the ASTM C1293 [15] grading. Specifications related to concrete aggregates for field concrete should consider the influence of aggregate grading on the ASR performance of concrete. Similar studies with a variety of reactive aggregates will further advance the understanding of the effect of coarse aggregate grading on the ASR performance of concrete.

Acknowledgements

The authors acknowledge the support from the Ministry of Transportation Ontario, Canada for providing the reactive Spratt aggregate; Lafarge Canada Inc. for providing the non-reactive Orillia sand; and Holcim Canada Inc. for providing the cement. The authors also acknowledge funding through a contract with Canadian Nuclear Safety

Commission (CNSC). Although financed by the CNSC, the contents of this paper reflect the views of the authors and they do not represent, in any case, the technical position of the CNSC. Thanks to Professor Karl Peterson for the help in acquiring UV images.

References

- [1] T. Ichikawa, Alkali-silica reaction, pessimum effects and pozzolanic effect, *Cem. Concr. Res.* 39 (2009) 716–726.
- [2] S. Multon, M. Cyr, A. Sellier, N. Leklou, L. Petit, Coupled effects of aggregate size and alkali content on ASR expansion, *Cem. Concr. Res.* 38 (2008) 350–359.
- [3] S. Multon, M. Cyr, A. Sellier, P. Diederich, L. Petit, Effects of aggregate size and alkali content on ASR expansion, *Cem. Concr. Res.* 40 (2010) 508–516.
- [4] C. Zhang, A. Wang, M. Tang, B. Wu, N. Zhang, Influence of aggregate size and aggregate size grading on ASR expansion, *Cem. Concr. Res.* 29 (1999) 1393–1396.
- [5] X.X. Gao, S. Multon, M. Cyr, A. Sellier, Alkali-silica reaction (ASR) expansion: pessimum effect versus scale effect, *Cem. Concr. Res.* 44 (2013) 25–33.
- [6] E. Garcia-Diaz, D. Bulteel, Y. Monnin, P. Degrugilliers, P. Fasseu, Pessimism behaviour of silicious limestone aggregates, 13th Int. Conf. Alkali-Aggregate React. Concr., Trondheim, 2008.
- [7] T.E. Stanton, Expansion of concrete through reaction between cement and aggregate, *Proc. Am. Soc. Civ. Eng.* 1940, pp. 1781–1811.
- [8] F. Rajabipour, E.R. Giannini, C.F. Dunant, J.H. Ideker, M.D.A. Thomas, Alkali-silica reaction: current understanding of the reaction mechanisms and the knowledge gaps, *Cem. Concr. Res.* 76 (2015) 130–146.
- [9] J. Lindgard, O. Andic-Cakir, I. Fernandes, T.F. Ronning, M.D.A. Thomas, Alkali-silica reactions (ASR): literature review on parameters influencing laboratory performance testing, *Cem. Concr. Res.* 42 (2012) 223–243.
- [10] H.W. Reinhardt, O. Mielich, A fracture mechanics approach to the crack formation in alkali-sensitive grains, *Cem. Concr. Res.* 41 (2011) 255–262.
- [11] C.F. Dunant, K.L. Scrivener, Effects of aggregate size on alkali-silica-reaction induced expansion, *Cem. Concr. Res.* 42 (2012) 745–751.
- [12] B.J. Wigum, Assessment and development of performance tests for alkali aggregate reaction in Iceland, 14th Int. Conf. Alkali Aggreg. React., Austin, Texas, USA 2012, p. 10.
- [13] W.J. French, Avoiding concrete aggregate problems, in: W.J. French (Ed.), *Improv. Civ. Eng. Struct. Old New*, Geotechnical Publishing Ltd, Basildon Essex, UK 1994, pp. 65–95.
- [14] ASTM C33, Standard Specification for Concrete Aggregates, ASTM International, West Conshohocken, PA, 2016.
- [15] ASTM C1293, Standard Test Method for Determination of Length Change of Concrete Due to Alkali-Silica Reaction, ASTM International, West Conshohocken, PA, 2015.
- [16] K.J. Lesnicki, J.-Y. Kim, K.E. Kurtis, L.J. Jacobs, Assessment of alkali-silica reaction damage through quantification of concrete nonlinearity, *Mater. Struct.* 46 (2013) 497–509.
- [17] R.D. Hooton, C. Rogers, C.A. MacDonald, T. Ramlochan, Twenty-year field evaluation of alkali-silica reaction mitigation, *ACI Mater. J.* 110 (2013) 539–548.
- [18] M.D.A. Thomas, B. Fournier, K.J. Folliard, J.H. Ideker, M.H. Shehata, Test methods for evaluating preventive measures for controlling expansion due to alkali-silica reaction in concrete, *Cem. Concr. Res.* 36 (2006) 1842–1856.
- [19] B. Fournier, J.H. Ideker, K.J. Folliard, M.D.A. Thomas, P.-C. Nkinamubanzi, R. Chevrier, Effect of environmental conditions on expansion in concrete due to alkali-silica reaction (ASR), *Mater. Charact.* 60 (2009) 669–679.
- [20] F. Habibi, S.A. Sheikh, N. Orbovic, D.K. Panesar, F.J. Vecchio, Alkali aggregate reaction in nuclear concrete structures part 3: structural wall element aspects, SMIRT23, Manchester, U.K., 2015.
- [21] P. Rangaraju, M. Balitsaris, H. Kizhakomudom, Impact of Aggregate Gradation on Properties of Portland Cement Concrete, Clemson, South Carolina, 2013.
- [22] B. Fournier, C.A. Rogers, C. MacDonald, Multilaboratory study of the concrete prism and accelerated mortar bar expansion tests with Spratt aggregate, 14th Int. Conf. Alkali Aggreg. React., Texas, USA 2012, p. 10.
- [23] C.A. Rogers, C.A. MacDonald, The geology, properties and field performance of alkali-aggregate reactive Spratt, Sudbury and Pittsburg aggregate distributed by the Ontario Ministry of Transportation, 14th Int. Conf. Alkali Aggreg. React., Texas, USA 2012, p. 10.
- [24] ASTM C78, Standard Test Method for Flexural Strength of Concrete (Using Simple Beam With Third-point Loading), ASTM International, West Conshohocken, PA, 2015.
- [25] P.E. Grattan-Bellew, Laboratory evaluation of alkali-silica reaction in concrete from Saunders Generating Station, *ACI Mater. J.* 92 (1995) 126–133.
- [26] V. Villeneuve, B. Fournier, J. Duchesne, Determination of the damage in concrete affected by ASR - the damage rating index (DRI), 14th Int. Conf. Alkali Aggreg. React. Concr., Texas, USA 2012, p. 10.
- [27] B. Fournier, P.-L. Fecteau, V. Villeneuve, S. Tremblay, L.F.M. Sanchez, Description of Petrographic Features of Damage in Concrete Used in the Determination of the Damage Rating Index (DRI), Laval University, Quebec City, Quebec, Canada, 2015.
- [28] H. Layssi, P. Ghods, A.R. Alizadeh, M. Salehi, Electrical resistivity of concrete: concepts, applications and measurement techniques, *Concr. Int.* 41–46 (2015).
- [29] FM 5-578, Florida Method of Test for Concrete Resistivity as an Electrical Indicator of Its Permeability (Tallahassee, Florida) 2004.
- [30] R.J. Kessler, R.G. Powers, E. Vivas, M.A. Paredes, Y.P. Virmani, Surface resistivity as an indicator of concrete chloride penetration resistance, 2008 Concr. Bridg. Conf., St. Louis, Missouri 2008, p. 18.

- [31] ASTM C1556, Standard Test Method for Determining the Apparent Chloride Diffusion Coefficient of Cementitious Mixtures by Bulk Diffusion, ASTM International, West Conshohocken, PA, 2016.
- [32] ASTM C1202, Standard Test Method for Electrical Indication of Concrete's Ability to Resist Chloride Ion Penetration, ASTM International, West Conshohocken, PA, 2012.
- [33] J. Tanesi, A. Ardani, Surface resistivity test evaluation as an indicator of the chloride permeability of concrete, FHWA-HRT-13-024 2012, pp. 1–6.
- [34] ASTM C597, Standard Test Method for Pulse Velocity Through Concrete, ASTM International, West Conshohocken, PA, 2009.
- [35] ASTM C469, Standard Test Method for Static Modulus of Elasticity and Poisson's Ratio of Concrete in Compression, ASTM International, West Conshohocken, PA, 2014.
- [36] ASTM C39, Standard Test Method for Compressive Strength of Cylindrical Concrete Specimens, ASTM International, West Conshohocken, PA, 2016.
- [37] A.E.K. Jones, L.A. Clark, The effects of ASR on the properties of concrete and the implications for assessment, *Eng. Struct.* 20 (1998) 785–791.
- [38] R.N. Swamy, M.M. Al-Asali, Engineering properties of concrete affected by alkali-silica reaction, *ACI Mater. J.* (1988) 367–374.
- [39] E.R. Giannini, Evaluation of Concrete Structures Affected by Alkali-Silica Reaction and Delayed Ettringite Formation (PhD thesis) The University of Texas at Austin, 2012.
- [40] B.P. Gautam, Multiaxially Loaded Concrete Undergoing Alkali-Silica Reaction (ASR) (PhD thesis) University of Toronto, 2016.
- [41] W. Elkey, E.J. Sellevold, Electrical Resistivity of Concrete, Oslo, Norway, 1995.
- [42] G. Charmchi, The Role of Concrete Maturity in Resistivity-based Performance Specifications (Master's Thesis) University of Toronto, 2015.
- [43] S. Preibisch, S. Saalfeld, P. Tomancak, Globally optimal stitching of tiled 3D microscopic image acquisitions, *Bioinformatics* 25 (2009) 1463–1465.